Thermal Decomposition of Hydrazines from Reactive Dynamics Using the ReaxFF Reactive Force Field

Luzheng Zhang,[†,‡] Adri C. T. van Duin,[†,§] Sergey V. Zybin,[†] and William A. Goddard III*[,†]

Materials and Process Simulation Center, Beckman Institute (139-74), California Institute of Technology, Pasadena, California 91125, The Petroleum Recovery Research Center, New Mexico Institute of Mining and Technology, Socorro, New Mexico 87801, and Department of Mechanical and Nuclear Engineering, Pennsylvania State University, University Park, Pennsylvania 16802

Received: January 8, 2009; Revised Manuscript Received: May 14, 2009

We report reactive dynamics (RD) studies on: the decomposition of bulk hydrazine (N_2H_4); the decomposition of bulk monomethyl-hydrazine ($CH_3N_2H_3$), hereafter referred to simply as methyl-hydrazine; the decomposition of hydrazine in the presence of hydrogen peroxide (H_2O_2); and decomposition hydrazine on catalytic surfaces Pt[100] and Pt[111] under various conditions. These studies use the ReaxFF reactive force field to describe the multitude of chemical reactions in these systems for a variety of reaction conditions in order to show that this approach leads to realistic decomposition mechanisms and rates. In particular, we determined how the decomposition of hydrazine is affected by temperature, pressure, and heating rate. We analyzed chemical reaction mechanism of the decomposition of hydrazine at the studied conditions and found that at lower temperatures the initial product from hydrazine decomposition is NH_3, whereas at higher temperatures H_2 and N_2 are the dominant early products. Prominent intermediates observed during these decompositions include N_2H_3, N_2H_2, and NH_2, in agreement with quantum mechanical studies (7.3 ps at 3000 K). As the heating rate is decreased, the onset for hydrazine decomposition shifts to lower temperatures. Using a constant heating rate, we found that higher pressure (increased density) favors formation of NH_3 over N_2 and H_2. In studies of the catalytic decomposition of hydrazine on surfaces Pt[100] and Pt[111], we found that the presence of a Pt-catalyst reduces the initial decomposition temperature of hydrazine by about 50%. We found that the Pt[100]-surface is 20 times more active for hydrazine decomposition than the Pt[111]-surface, in qualitative agreement with experiments. These studies indicate how ReaxFF RD can be useful in understanding the chemical processes involved in bulk and catalytic decomposition and in oxidation of reactive species under various reaction conditions.

1. Introduction

Chemical processes play an essential role in many areas of technology, but often the systems are too complex to extract from experiments a fundamental understanding of the atomistic mechanism underlying the chemical processes. For example, in the design of rocket engines and satellite thrusters it is important to know the detailed chemical reaction mechanisms occurring at the reaction fronts of such energetic materials as hydrazines at the high densities and temperatures involved in combustion or detonation conditions.[1−4] Numerous chemical reaction steps have been proposed, but it has been very difficult to extract from experiments the details necessary to determine which steps actually occur and their relative importance. Progress has been made by using quantum mechanics (QM) to examine the energetic barriers for particular reaction steps, but it is generally not possible to apply such QM to the systems with many thousands of atoms exposed to a variety of temperature and pressure transients for sufficient times to characterize the dynamic processes in combustion or detonation.

Hydrazine is an important ingredient in many propellants, producing a large amount of heat when burned, having mainly N_2 and H_2O as final products. It can also be used without an oxidant, in which case it decomposes into NH_3, N_2, and H_2. The energy output of oxidant-free hydrazine decomposition is about six times lower than that of hydrazine oxidation. Oxygen-free hydrazine decomposition can be initiated using such catalyst surfaces as Pt.[1−3]

The general set of reactions involved in the decomposition of hydrazine has been discussed in ref 1. Diesen[5] used mass spectroscopy to study the kinetics behind the shock wave of hydrazine diluted in argon over a temperature range of 1200−2500 °C and determined the overall rate constant within this temperature range. Konnov and De Ruyck[6] developed a detailed N/H reaction mechanism, consisting of 51 reactions for 11 species. This mechanism was validated by comparing kinetic modeling results with measurements of hydrazine pyrolysis in shock waves and in hydrazine decomposition flames at low and atmospheric pressures. The overall calculated rate of decomposition by this mechanism agrees well with experiments for pure hydrazine and its mixtures with argon, nitrogen, water, and ammonia. Other kinetic mechanisms were reported in refs 7−10.

The catalytic decomposition of hydrazine on metal surfaces (Pt, Ni, Cd, and Ir/Al_2O_3) and supported metal particles (Ir/Al_2O_3) has been investigated experimentally for years,[1−3,11−19] and simplified reactions mechanisms have been proposed for various surfaces.

* Corresponding author. Phone: (626) 395-2731; fax: (626) 585-0918; e-mail: wag@wag.caltech.edu.
† California Institute of Technology.
‡ New Mexico Institute of Mining and Technology.
§ Pennsylvania State University.

10.1021/jp900194d CCC: $40.75
Published on Web 07/14/2009

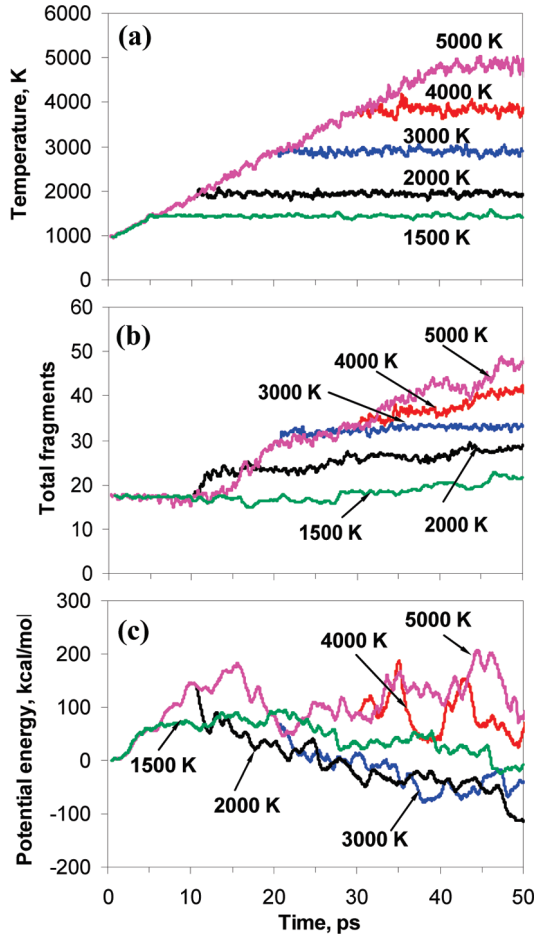

Figure 1. Results from ReaxFF RD of bulk hydrazine (18 molecules in a cube of side 12.0 Å, (density = 0.554 g/cm^3) heated to 1500, 2000, 3000, 4000, and 5000 K at a heating rate of 100 K/ps; (a) system temperature, (b) total fragments, and (c) potential energy change.

We propose here an alternative approach to studying the combustion and reaction properties in complex dynamic systems with reactive dynamics (RD) simulations using the ReaxFF reactive force field and demonstrate its application.

To evaluate how well ReaxFF can describe the high-temperature behavior of hydrazine, we performed RD simulations of bulk hydrazine (N_2H_4) and bulk methyl-hydrazine ($CH_3N_2H_3$) under various temperature and pressure conditions. We also simulated the reactions of hydrazine in the presence of hydrogen peroxide (H_2O_2) and on catalytic surfaces Pt[100] and Pt[111]. These simulations provide detailed atomistic-scale information on the chemical events occurring under various thermal and pressure conditions. We also studied how the decomposition of hydrazine depends on temperature, density/pressure, and heating rate.

We find that the results from ReaxFF simulations are in reasonable agreement with the results available from previous experimental and theoretical studies. This suggests that such RD simulations might be useful to improve the performance of hydrazine-based jet and rocket fuels, where an understanding of chemical events related to hydrazine decomposition is required.

2. The ReaxFF Reactive Force Field

2.1. Overview of ReaxFF. The ReaxFF reactive force field was developed to reproduce QM energies for a large variety of reaction pathways involving reaction intermediates and transition-state structures.[20−26] The parameters in ReaxFF are adjusted to reproduce the energetics and reactive surfaces found with QM for a number of prototypical calculations and then used for system sizes, temperature, pressures, and reaction times far too large for QM; ReaxFF has been practical to apply to the study of the high-temperature dynamics of chemically reactive systems, providing an atomistic-scale description of the decomposition of high-energy material.[20,21,26]

2.2. Definition of ReaxFF. ReaxFF allows the valence interactions (bonds, angles, torsions) and charges to change continuously as bonds form and break in reactions. The instantaneous bond orders are determined from the bond distances that in turn determine the forces. ReaxFF includes the concept of valence so that there are forces that encourage the instantaneous bond orders to be consistent with the valence. These bond orders are updated at every RD iteration, allowing ReaxFF to recognize the formation of new bonds and the dissociation of existing bonds. In addition, there is a general algorithm for specifying the instantaneous charges on each atom so that they can redistribute as the molecules react. The electrostatic and van der Waals (vdW) nonbond energies act between all pairs of atoms (even bonded ones) so that there are no discontinuous changes as bonds are formed and broken.

The energy function for ReaxFF has the form:

$$E_{system} = E_{bond} + E_{over} + E_{under} + E_{val} + E_{pen} + E_{tors} + E_{conj} + E_{vdW} + E_{Coulomb}$$

where bond-order dependent terms include bond energies, valence angle, lone pair, conjugation, and torsion angle to describe the valence forces arising from molecular orbitals, and the nonbond terms (independent of bond-order) handle vdW and Coulomb interactions. ReaxFF can describe organic, inorganic, and metallic materials and interfaces between them, with parameters that can be fitted to one system and applied to another (transferable). The major goal in the development of the ReaxFF was to obtain a transferable force field that can describe the energy surfaces and coordination changes associated with reactions while simultaneous describing ground state structures correctly. Indeed ReaxFF has been successfully applied the ReaxFF to many systems.[20−27]

The ReaxFF parameters used herein were parametrized previously against a training set of QM-derived data that combined the properties of numerous H/C/N/O-containing compounds (bond dissociation, geometry distortion, IR-spectra, condensed phase properties) with a wide range of reactions for nitramine-[20,21] and peroxide-based[27] high-energy materials. In particular, ref 20 validated the ReaxFF for describing N/H processes. This includes cases involving N−N single, double, and triple bond dissociation and involving H−N−H, H−N−N, and N−N−N angle strain relations as along with H−H bond dissociation. These validations provide support for the reaction mechanism described in this paper.

For the simulations on hydrazine/Pt we combined ReaxFF parameters with a recently developed ReaxFF description for H/C/O/N interactions with Pt, which had been tested against Pt-bulk and surface properties and binding energies for H/C/O/N-containing compounds to Pt-atoms and Pt-surfaces.

Except for the H_2N-NH_2 and HN═NH bond dissociation profile (which had already been part of the basic H/C/N/O QM-training set), no hydrazine-specific data was included in the ReaxFF parametrization. Thus, these results indicate the transferability of the ReaxFF. For more details about ReaxFF, see

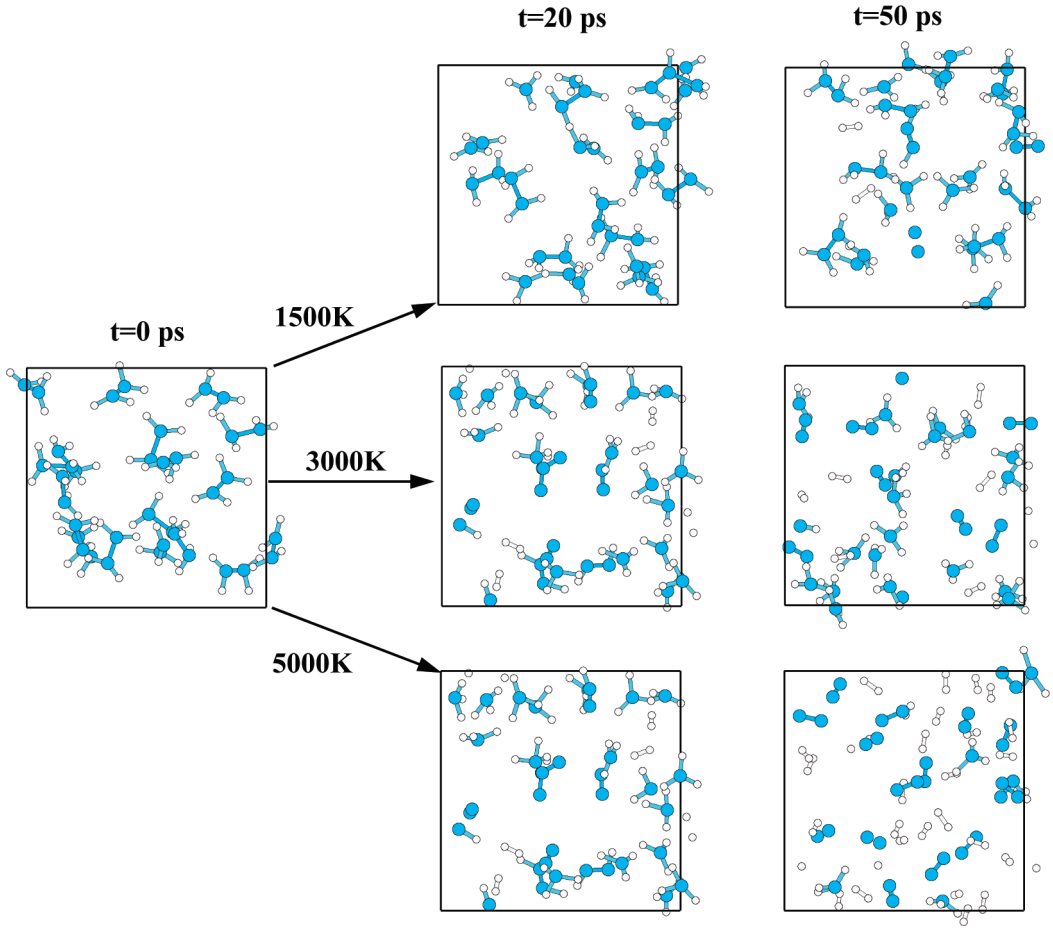

Figure 2. Snapshots at $t = 0$, 20, and 50 ps for bulk hydrazine (same as in Figure 1, with density = 0.554 g/cm^3) heated to 1500, 3000, and 5000 K at a heating rate of 100 K/ps.

van Duin et al.[22,23] For completeness, all ReaxFF parameters used in these simulations are included in the Supporting Information.

3. Simulation Details

The systems studied in this work are hydrazine (H_2N-NH_2) in the bulk phase, in the presence of hydrogen peroxide (H_2O_2) and in contact with Pt surfaces, plus methyl-hydrazine [$CH_3(HN)-NH_2$] in the bulk phase.

For bulk phase hydrazine, we carried out a number of independent simulations for 18, 24, 33, or 40 molecules per periodic cell. These were placed in a cubic simulation box, 12.00 Å on a side, leading to four initial hydrazine systems with densities of 0.554, 0.739, 1.016, and 1.232 g/cm^3. These bulk densities are near the experimental liquid density of 1.01 g/cm^3 at room temperature.

For bulk methyl-hydrazine we placed 20 molecules in a cubic simulation box 12.05 Å on a side box, resulting in a density 0.874 g/cm^3, close to the experimental density of 0.88 g/cm^3.

For the system of hydrazine in the presence of hydrogen peroxide, we placed a mixture of 18 N_2H_4 molecules with 9 H_2O_2 molecules in a cubic simulation box of side 12.00 Å.

For the hydrazine on Pt surfaces, we placed 36 hydrazine molecules in a periodic box containing a two-dimensional periodic slab exposing Pt[100] or Pt[111] surfaces, with a box size that leads to a hydrazine density of 0.554 g/cm^3. The dimensions of the simulation box were (21.11 Å × 11.77 Å × 11.77 Å) for hydrazine on Pt[100] and (22.54 Å × 14.42 Å × 11.10 Å) for hydrazine on Pt[111]. Both Pt surfaces were obtained from the zero-pressure Pt fcc-crystal structure and contained six layers of Pt atoms along the z-direction. That led to 90 Pt-atoms per cell for Pt[100] and 120 Pt-atoms per cell for Pt[111].

All systems were minimized and equilibrated for 4.0 ps at specified temperatures (1000 K in most cases) using ReaxFF RD simulations (NVT) with the Berendsen-thermostat (damping constant = 50 fs) to control the temperature. The 1000 K-equilibrated systems were then used to perform NVT or NVE RD simulations for 50−80 ps.

In all simulations, the RD time step was set to 0.10 fs and the bond order cutoff for molecule recognition was set at 0.3. This bond-order cutoff is used only for analysis purposes and does not affect the ReaxFF energy or force calculation.

During the cook-off simulations, the system temperature, potential energy, the number of fragments and molecule trajectory were recorded every 0.25 fs. Species analysis for each system was done based on the trajectory.

4. Results and Discussions

4.1. Temperature Effects. ***4.1.1. Potential Energy and Total Fragments.*** We first performed RD simulations on the system of bulk hydrazine with a density of 0.554 g/cm^3. The system was started at 1000 K, heated to 1500, 2000, 3000, 4000, and 5000 at a rate of 100 K/ps, and then kept constant at these temperatures. The total simulation lasted 50 ps. Figures 1a−c give the system temperature, total number of fragments and potential energy change during such thermal conditions, respectively.

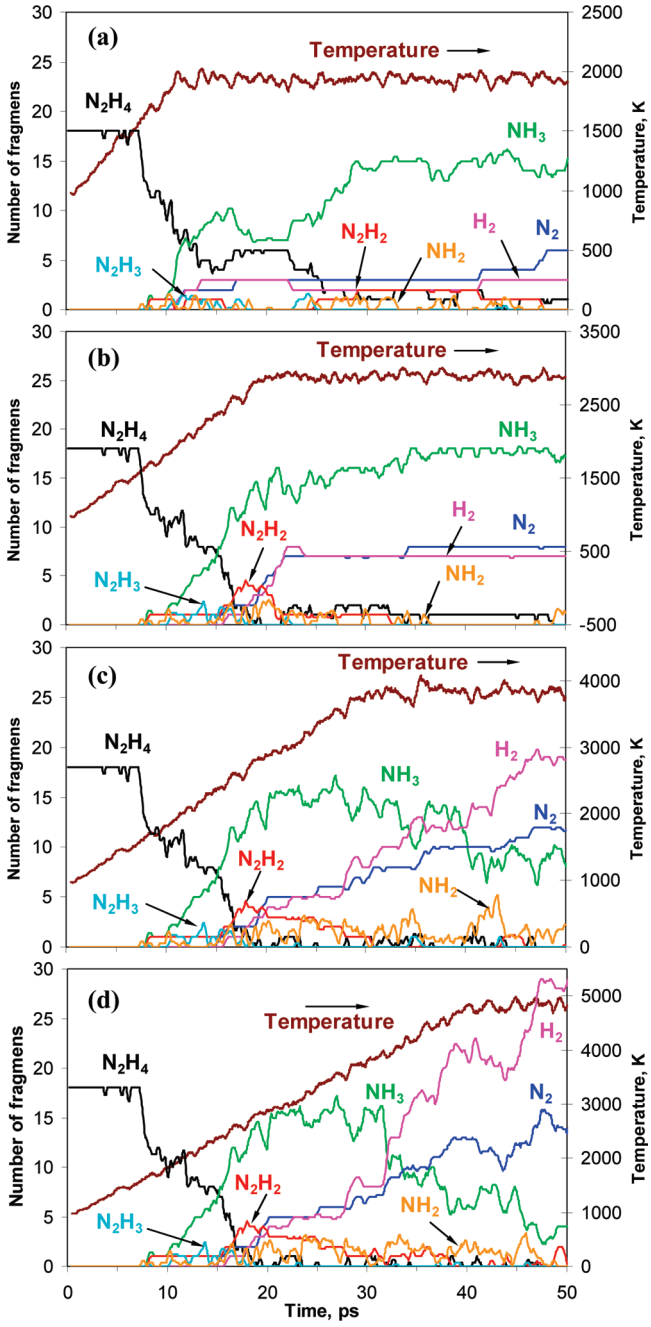

Figure 3. Species analyses for the decomposition of bulk hydrazine (same as in Figure 1, with density = 0.554 g/cm^3) heated to 2000, 3000, 4000, and 5000 K at a heating rate of 100 K/ps.

At 1500 K, we found that hydrazine molecule just begins to decompose at 50 ps, whereas they start to decompose at 7.3 ps for other cases (2000, 3000, 4000, and 5000 K). The total number of fragments formed in the whole cookoff process increases with temperature (Figure 1b). At 50 ps, the average number of fragments generated for each initial hydrazine molecule is 1.61 (2000 K), 1.83 (3000 K), 2.28 (4000 K), and 2.78 (5000 K), indicating the increased decomposition of hydrazine with temperature. The rate of hydrazine loss with temperature is plotted in Figure 3, where we see an effective activation temperature of around 1550 K (see below). The corresponding potential energies, as plotted in Figure 1c, for these systems heated to 1500, 2000, 3000, 4000, and 5000 K show that hydrazine molecules gain energy from the heating (before 10 ps) and start to decompose. With the decomposition of hydrazine molecules, the potential energy basically decreases.

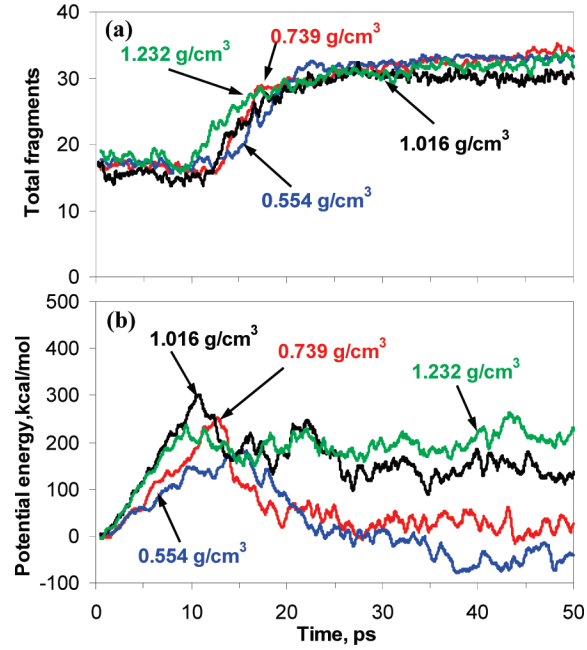

Figure 4. Results from ReaxFF RD of bulk hydrazine at various densities (0.554, 0.739, 1.016, and 1.232 g/cm^3) heated from 1000 to 3000 K at a heating rate of 100 K/ps; (a) total fragments and (b) potential energy change.

Snapshots at $t = 0$, 20, and 50 ps from these simulations are shown in Figure 2. This shows that many hydrazine molecules remain intact at 1500 K, and all hydrazine molecules decompose by 50 ps for temperatures 3000 and 5000 K with formation of many NH_3, N_2, and H_2 species.

4.1.2. Species Analysis. Figure 3 shows the species analysis of hydrazine heated to temperatures ranging from 2000 to 5000 K (no species analysis was done at 1500 K since almost no N_2H_4 molecules decomposed). We found that N_2H_4 molecules start to decompose at ~7.3 ps ($T \approx 1550$ K), at which point the hydrazine molecules dissociate very quickly, resulting in NH_3 products and NH_2, N_2H_3, and N_2H_2 intermediates. The products N_2 and H_2 start forming at ~10.8 ps and continue increasing until reactions in the system reach equilibrium. At temperatures of 2000 and 3000 K, the concentration of N_2 and H_2 becomes stable after 13.5 and 24.0 ps, respectively, while it continues to increase after 50 ps RD simulations at 4000 and 5000 K.

All the fragments observed in our simulations (NH_2, N_2H_3, N_2H_2, NH3, N_2, and H_2) have been observed experimentally in the steady-state chain reaction mechanism,[5] indicating that ReaxFF leads to a plausible description of hydrazine thermal decomposition.

Our results show that the primary reaction product of hydrazine decomposition is NH_3, which at elevated temperatures is converted into the entropically more favorable H_2 and N_2.

4.1.3. Reaction Mechanism. To accurately model the decomposition of hydrazine, either the decomposition mechanisms or the kinetics of the reactions that are involved are required. But only a few initial decomposition reaction rates and a few rate constants for hydrazine reacting with atoms and radicals have been measured.[5−9]

In this study we simulated the decomposition of hydrazine molecules under various conditions and demonstrate the effect of various factors (temperature, pressure, etc.) on the decomposition reaction. In the meantime, we analyzed the decomposition mechanism by tracking the trajectories of species in the systems involved in the decomposition.

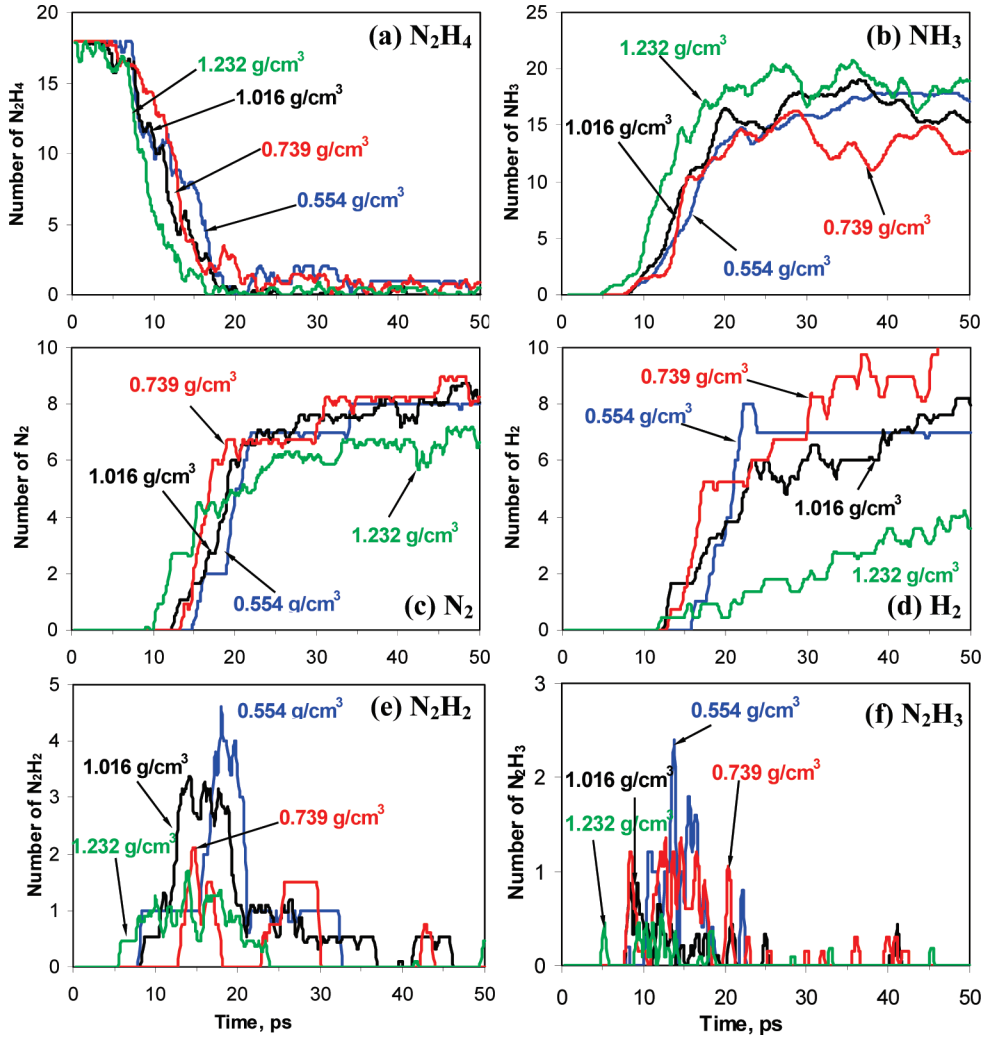

Figure 5. Comparisons of species produced in ReaxFF RD decomposition of bulk hydrazine at various densities (0.554, 0.739, 1.016, and 1.232 g/cm^3) heated to 3000 K at a heating rate of 100 K/ps; (a) hydrazine (N_2H_4), (b) NH_3, (c) N_2, (d) H_2, (e) N_2H_2, and (f) N_2H_3.

We first analyzed the reaction mechanism for the decomposition of hydrazine at a typical decomposition temperature of 3000 K (NVT). We found that N_2 and H_2 form with N and H elements from either the same hydrazine or different hydrazine molecules. As the temperature increases, the decomposition leads to various molecules.

During the early stages most of the formation of NH_3, is from the same hydrazine molecule, that is, $N_2H_4 \rightarrow N_2H_3 + H$ and $N_2H_3 \rightarrow NH_3 + H_2$. This result is similar to the results in the literature.[5,10] As the decomposition temperature is increased, the newly formed NH_3 molecules react with other molecules or intermediates to form N_2, H_2, and additional NH_3. Here the collisions at high temperature result in decomposition of products to form new species (secondary chemical reactions) during the decomposition). We observed the hydrogen abstraction reaction $N_2H_4 + H \rightarrow N_2H_3 + H_2$ during the decomposition of hydrazine molecules under these conditions, as previously mentioned by Li et al.[10]

A similar trend on the decomposition mechanism is observed in the cases of hydrazine systems heated at different rates. At a high heating rate, hydrazine molecules are accelerated to high speed and have more collisions, similar to the case with high decomposition temperature.

4.2. Density/Pressure Effects. ***4.2.1. Potential Energy and Total Fragments.*** We also studied the effect of density/pressure on the decomposition of bulk hydrazine. Figures 4a−b give the total fragments and the potential energy changes for the systems with the densities 0.554, 0.739, 1.016, and 1.232 g/cm^3. These systems were heated from 1000 to 3000 K at a rate of 100 K/ps, and then the temperature was kept at constant at 3000 K. Figure 4a shows that increasing density leads to an earlier initiation of decomposition (7.3 ps at 0.554 g/cm^3 vs 5.0 ps at 1.016 g/cm^3), but the effect of density on hydrazine decomposition is much less than that of temperature. Potential energies for these systems increase with temperatre at constant volume (see Figure 4b) until ~10 ps, where it starts decreasing due to the decomposition.

4.2.2. Species Analysis. Figures 5a−f show the number of N_2H_4, NH_3, N_2, H_2, N_2H_2, and N_2H_3 fragments observed at various densities. At all densities, the hydrazine molecules decompose very quickly, leading to final products N_2, H_2, and NH_3 along with intermediates NH_2, N_2H_3, and N_2H_2. Figure 5a shows that the decomposition of hydrazine molecules starts slightly earlier at high density (1.232 g/cm^3) than at the other densities. We also found that NH_3 is more dominant at high density. This suggests that the secondary reactions leading to N_2 and H_2 formation are repressed at higher densities.

4.3. Heating Rate Effects. To test the influence of heating rate on the decomposition of hydrazine, we performed RD simulations starting with hydrazine at a density of 0.554 g/cm^3, but heating to 3000 K at various heating rates: 50, 100, and 200 K/ps followed by constant temperature RD at 3000 K. The system temperature, total fragments formed in the decomposi-

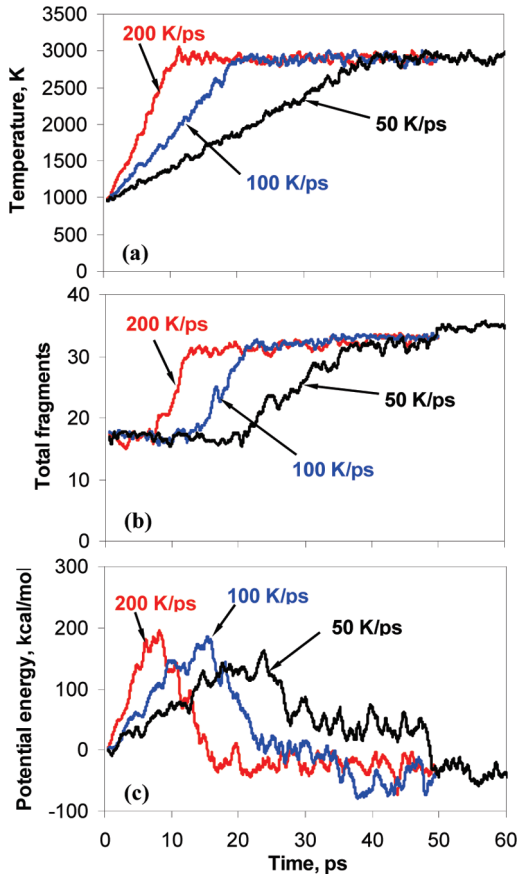

Figure 6. Comparisons of ReaxFF RD results for decomposition of bulk hydrazine at density 0.554 g/cm^3 heated to 3000 K at various heating rates; (a) system temperature, (b) total fragments, and (c) potential energy change.

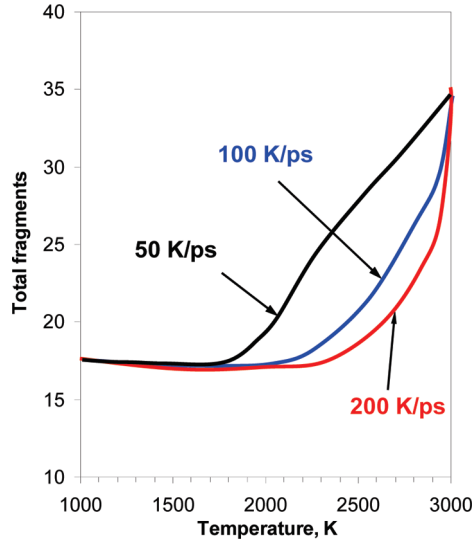

Figure 7. Total fragments from ReaxFF RD decomposition of bulk hydrazine at density 0.554 g/cm3 heated from 1000 to 3000 K at various heating rates.

tion, and the potential energy change are shown in Figures 6a−c. In all three cases hydrazine molecules decompose and new fragments are formed (Figure 6b), but the time at which hydrazine starts to decompose varies. The maximum in potential energy, marking the point where the exothermic reactions begin to occur, is higher for the faster heating rates (Figure 6c).

Figure 7 shows the average number of species as a function of system temperature for the various heating rates. We observed

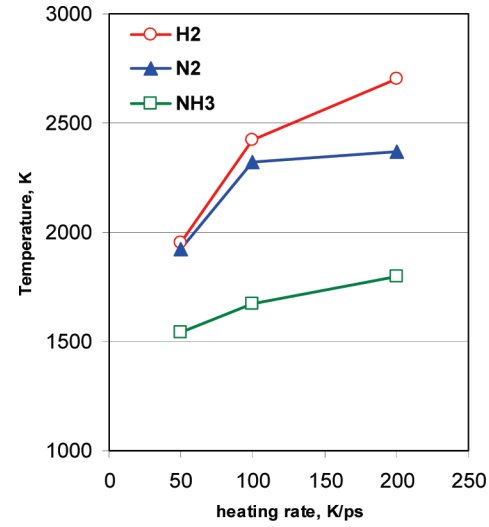

Figure 8. The threshold temperature at which the first formation of H_2, N_2, and NH_3 molecules is observed in ReaxFF RD decomposition of bulk hydrazine at a density of 0.554 g/cm^3 and heated from 1000 to 3000 K at various heating rates.

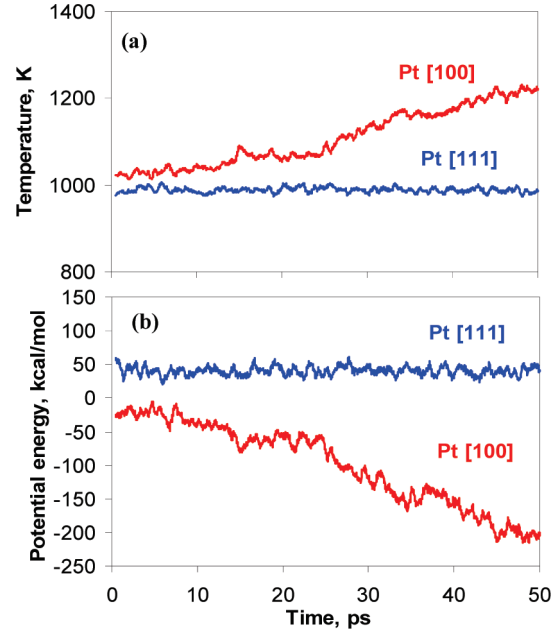

Figure 9. Comparisons of the decomposition of bulk hydrazine (density = 0.554 g/cm^3) on surfaces Pt[100] and Pt[111] from NVE RD simulations starting at 1000 K; (a) system temperature and (b) potential energy change.

that the decomposition starts earlier for lower heating rates than that for higher heating rates. The total fragments starts to increase at 1820 K for 50 K/ps, 2100 K for 100 K/ps, and 2350 K for 200 K/ps. The simulation results also show that the first hydrazine molecule starts to decompose at around 1350 K for 50 K/ps, 1500 K for 100 K/ps, and 1690 K for 200 K/ps. The temperature threshold at which the first products NH_3, N_2, and H_2 appear for the systems under different heating rates is shown in Figure 8.

4.4. Hydrazine on Catalyst Surfaces. We found that bulk hydrazine does not decompose at 1000 K on the time scales employed in our simulations. To test the role of catalytic decomposition reactions of hydrazine, we performed NVE RD simulations of hydrazine molecules in the presence of Pt surfaces after the system was preheated to 1000 K for 4.0 ps.

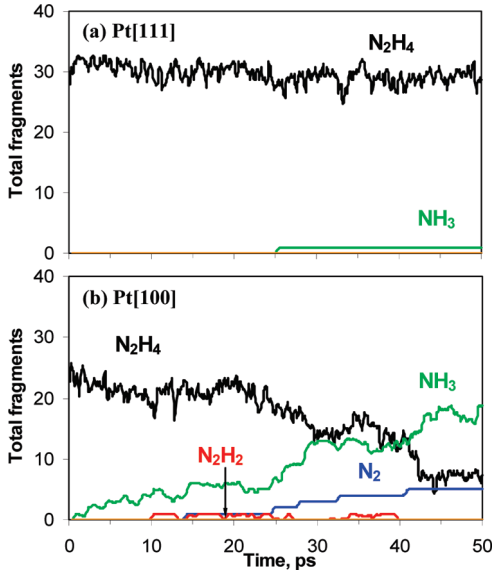

Figure 10. Species analyses for decomposition of bulk hydrazine (density = 0.554 g/cm^3) on surfaces of Pt[100] and Pt[111] from NVE RD simulations starting at 1000 K. Pt[100] is 20 times more reactive than Pt[111].

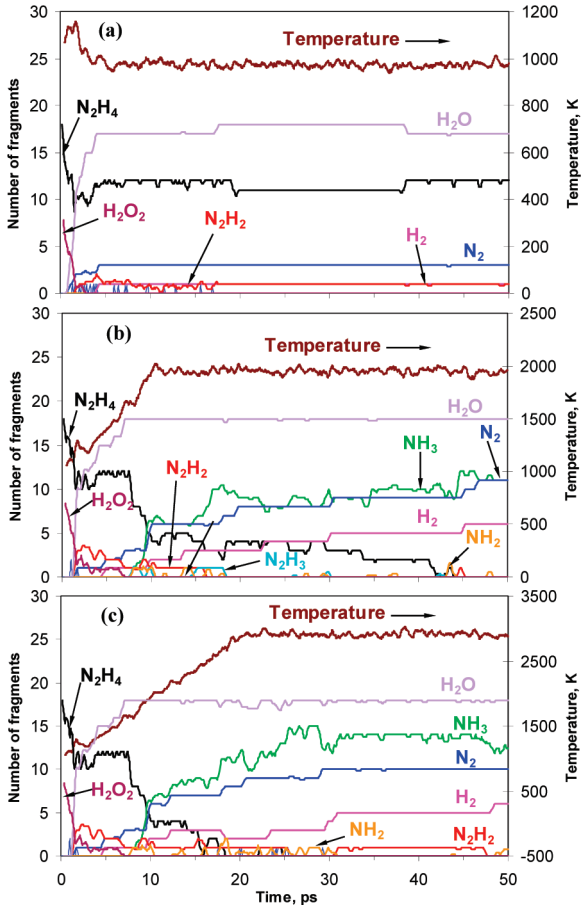

Figure 11. Species analyses for the decomposition of hydrazine in the presence of hydrogen peroxide heated to various temperatures; (a) 1000 K, (b) 2000 K, and (c) 3000 K at a rate of 100 K/ps. Temperature profiles are also displayed. In each case the cubic box of side 12.0 Å has 18 molecules of N_2H_4 and 9 molecules of H_2O_2.

Figures 9a−b give the system temperature and the potential energy evolution during the NVE RD simulations staring at 1000 K. We see that the Pt[111] surface has little impact, with the system temperature remaining around 1000 K, while the

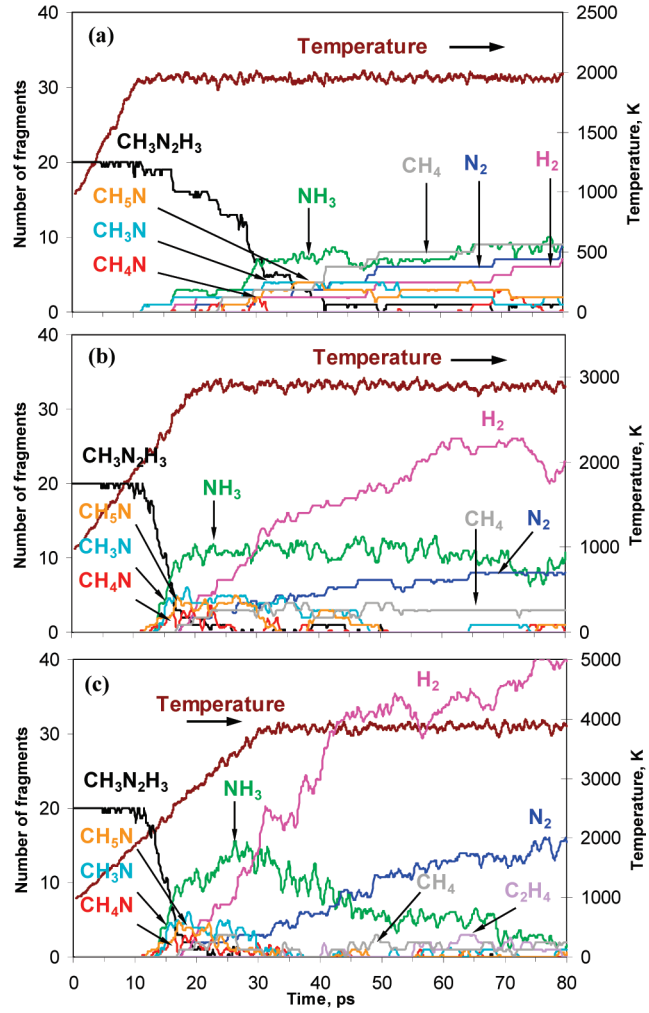

Figure 12. Species analyses for the decomposition of methyl-hydrazine (density = 0.874 g/cm^3) heated to (a) 2000 K, (b) 3000 K, and (c) 4000 K at a rate of 100 K/ps. Temperature profiles are also displayed.

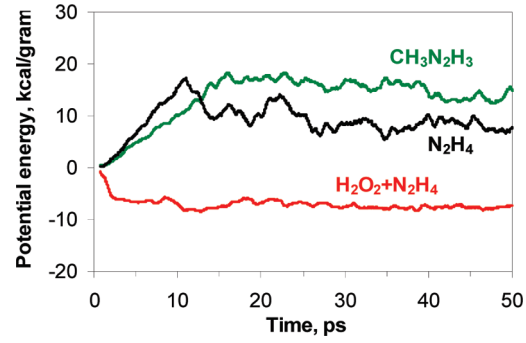

Figure 13. Potential energy change for the systems hydrazine (N_2H_4), methyl-hydrazine ($CH_3N_2H_3$), and hydrazine containing hydrogen peroxide (H_2O_2 + N_2H_4) heated to 3000 K at a rate of 100 K/ps.

exothermic reactions taking place on the Pt[100] surface leads to an increase to 1272 K within 50 ps. This decomposition of hydrazine on Pt[100] decreases the potential energy by 169 kcal/mol, while it remains constant for hydrazine on Pt[111].

Figure 10 gives detailed information on the intermediates and products during the catalytic decomposition of hydrazine on Pt surfaces.

For the Pt[111] surface, we found that no hydrazine molecules decompose until t = 25 ps.

The Pt[100] surface is far more reactive than Pt[111], leading to production of ~5 NH_3 molecules by 25 ps and ~20 NH_3 by 50 ps. Indeed, two-thirds of the hydrazines have decomposed on Pt[100] by ~40 ps. We observe formation of NH_3 plus such secondary reaction products as H_2 and a small amount of N_2H_2 molecules and H atoms chemisorbed on the Pt[100] surface. We see no nitrogen atoms chemisorbed on the Pt surface, indicating that nitrogen is formed via an intramolecular process, as observed by Ranney et al.[19]

These NVE RD simulations indicate that in the presence of the Pt[100] catalyst, the threshold temperature for hydrazine decomposition by 50 ps is reduced to below 1000 K. Indeed the decomposition of hydrazine on Pt[100] can initiate within 50 ps, even at 800 K. This decrease of the hydrazine decomposition temperature by the Pt catalyst agrees qualitatively with experimental results,[19,20] which found that decomposition temperature increases when the catalyst Pt surface is covered by CO molecules.

4.5. Hydrazine/Peroxide Mixtures. We also performed three simulations in which hydrogen peroxide (H_2O_2) molecules were mixed with hydrazine (with a N_2H_4/H_2O_2 ratio of 2:1). Starting at 1000 K the mixture was heated at a rate of 100 K/ps until it reached a constant temperature of 1000, 2000, and 3000 K, after which it was kept constant.

A detailed species analysis for the three temperatures in Figure 11 shows that hydrazine decomposition in the presence of peroxide occurs readily at 1000 K. This decomposition results from hydroxide radicals derived from peroxide dissociation extracting H from the hydrazine to form water molecules. By 4 ps, the H_2O_2 is gone with little further decomposition of the hydrazine molecules (the number of N_2H_4, H_2O, N_2, and H_2 remains constant).

For the system to be the heated to 2000 K, we observe a similarly early decomposition of hydrazine molecules facilitated by the presence of hydrogen peroxide. Within ~4 ps, every OH radical from H_2O_2 is consumed to form H_2O. As a result, the hydrazine decomposition stops because at this temperature the rate of pure thermal decomposition of hydrazine molecules is too low. However, after heating the system further to 1550 K ($t = 7.8$ ps), the remaining hydrazine molecules start to decompose quickly, leading to the end of the N_2H_4 plateau in Figure 11. The further, mainly thermal, decomposition generates substantially more N_2 and H_2, as well as new species such as NH_3 and N_2H_2 that are not observed in the 1000 K peroxide/hydrazine mixture simulation.

For the case of heating to 3000 K, the decomposition process leads to a hydrazine plateau at early times ($t < 7.8$ ps) similar to that at 2000 K, but the decomposition occurs much faster. In addition, although more NH_3 molecules are produced right away after 7.8 ps at 3000 K in comparison with the 2000 K case, they start to decompose later.

4.6. Decomposition of Methyl-hydrazine. Methyl-hydrazine (denoted as $CH_3N_2H_3$ in Figures 12 and 13) is frequently used in propellant compositions because it is more stable than hydrazine and performs better at the freezing point (as in spacecraft propulsion applications).[1] It is usually mixed with hydrazine for better performance.

We carried out NVT RD simulations on methyl-hydrazine with a density of 0.874 g/cm^3. Starting from 1000 K, the system was heated at a rate of 100 K/ps until temperatures of 2000, 3000, or 4000 K were attained, after which the temperature was kept constant. Figure 12 displays a detailed species analysis for these systems, which indicates that increasing the temperature leads to faster and more complete decomposition of methyl-hydrazine, with increased intermediates and products formed.

Figure 13 compares the potential energy change for the systems of hydrazine, hydrazine/peroxide, and methyl-hydrazine under the same conditions (heated to 3000 K at 100 K/ps). It shows that the presence of the oxidizer (H_2O_2) leads to a much more rapid decrease in the potential energy, indicating formation of more stable products, as shown in fragment analysis for these systems in Figures 3, 11, and 12. For hydrazine and methyl-hydrazine systems under the same thermal conditions, the methyl-hydrazine requires more energy to decompose, in agreement with the suggestions by Kerr et al.[28]

5. Conclusions

We present reactive dynamics (RD) simulations using the ReaxFF reactive force field to examine the decomposition of bulk hydrazine (N_2H_4), methyl-hydrazine ($CH_3N_2H_3$), hydrazine in the presence of hydrogen peroxide (H_2O_2), and on catalytic surfaces Pt[100] and Pt[111] under various conditions of temperature, density/pressure, and heating rate. These results provide information on the mechanism and chemical events during the decomposition of these hydrazines. The intermediates observed in the RD agree with results from previous experimental and QM studies. This demonstrates the applicability of ReaxFF for describing complex chemical systems under high-temperature conditions. Thus, ReaxFF RD simulations may be useful for studying the performance of propellants such as hydrazines.

We observed that both the temperature and the heating rate strongly affect the decomposition of hydrazine. At lower temperatures hydrazine decomposition primarily results in formation of NH_3, while at more elevated temperatures the secondary reaction products H_2 and N_2 begin to dominate. We identified various reaction intermediates (N_2H_3, N_2H_2 and NH_2) from our ReaxFF simulations. We also found that an increase in density results in a suppression of H_2 and N_2 formation. A brief reaction mechanism was analyzed for the decomposition of hydrazine in the bulk and on Pt surface.

We found that the decomposition temperature of hydrazine decreases significantly in the presence of [100] and [111] Pt surfaces, with Pt[100] being more active. This indicates that ReaxFF can describe the Pt-catalyzed hydrazine decompositions. These results agree with experimental findings. These simulations suggest that ReaxFF is capable of describing the high-temperature chemistry of hydrazine and hydrazine-related compounds.

Acknowledgment. This research was funded partly by ARO (MURI W911NF-05-1-0345 and W911NF-08-1-0124), ONR (N00014-05-1-0778 and N00014-09-1-0634), DOE-LANL (DE-AC52-06NA25396), and DARPA-PROM (N00014-02-1-0839). In addition, the computational facilities used in these studies were funded by ARO-DURIP and ONR-DURIP.

Supporting Information Available: This material is available free of charge via the Internet at http://pubs.acs.org.

References and Notes

(1) Schmidt, E. *Hydrazine and Its Derivatives: Preparation, Properties and Applications*; Wiley: New York, 1984.
(2) Soares Neto, T. G.; Cobo, A. J. G.; Cruz, G. M. *Appl. Catal., A* **2003**, *250*, 331.
(3) Vieiraa, R.; Bastos-Nettob, D.; Ledouxa, M.-J.; Pham-Huu, C. P. *Appl. Catal., A* **2005**, *279*, 35.
(4) Cooper, P. W. *Explosive Engineering*; Wiley: New York, 1996.
(5) Diesen, R. W. *J. Chem. Phys.* **1963**, *39*, 2121.

(6) Konnov, A. A. De Ruyck. *J. Combust. Flame* **2001**, *124*, 106.
(7) Miller, J. A.; Smooke, M. D.; Green, R. M.; Kee, R. J. *Combust. Sci. Technol.* **1983**, *34*, 149.
(8) Catoire, L.; Luche, J.; Dupre, G.; Paillard, C. *Shock Waves* **2001**, *11*, 97.
(9) Moberly, W. H. *J. Phy. Chem.* **1962**, *66*, 366.
(10) Li, Q. S.; Zhang, X.; Zhang, S. W. *J. Phys. Chem. A* **2003**, *107*, 6055.
(11) Alberas, D. J.; Kiss, J.; Liu, Z.-M.; White, J. M. *Surf. Sci.* **1992**, *278*, 51.
(12) Contour, J. P.; Pannetier, G *J. Catal.* **1972**, *24*, 434.
(13) Dopheide, R.; Schröter, L.; Zacharias, H. *Surf. Sci.* **1991**, *257*, 86.
(14) Ranney, J. T.; Gland, J. L. *Surf. Sci.* **1996**, *360*, 112.
(15) Carabineiro, S. A. C.; Nieuwenhuys, B. E. *Surf. Sci.* **2003**, *87*, 532.
(16) Chen, X.; Zhang, T.; Xia, L.; Li, T.; Zheng, M.; Wu, Z.; Wang, X.; Wei, Z.; Xin, Q.; Li, C. *Catal. Lett.* **2002**, *79*, 21.
(17) de Medeiros, J. E.; Valenca, G. P. Braz. *J. Chem. Eng.* **1998**, *15*, 104.
(18) Lee, S.; Fan, C.; Wu, T.; Anderson, S. L. *J. Phys. Chem.* **2005**, *109*, 381.
(19) Ranney, J. T.; Franz, A. J.; Gland, J. L. *Langmuir* **1997**, *13*, 2731.
(20) Strachan, A.; van Duin, A. C. T.; Chakraborty, D.; Dasgupta, S.; Goddard III, W. A. *Phys. Rev. Lett.* **2003**, *91*, 09301.
(21) Strachan, A.; Kober, E.; van Duin, A. C. T.; Oxgaard, J.; Goddard III, W. A. *J. Chem. Phys.* **2005**, *122*, 054502.
(22) van Duin, A. C. T.; Dasgupta, S.; Lorant, F.; Goddard, W. A. *J. Phys. Chem. A* **2001**, *105*, 9396.
(23) van Duin, A. C. T.; Strachan, A.; Stewman, S.; Zhang, Q.; Xu, X.; Goddard III, W. A. *J. Phys. Chem. A* **2003**, *107*, 3803.
(24) Zhang, Q.; Cagin, T.; van Duin, A. C. T.; Goddard III, W. A.; Qi, Y.; Hector, L. *Phys. Rev. B* **2004**, *69*, 045423.
(25) Nielson, K.; van Duin, A. C. T.; Oxgaard, J.; Deng, W.; Goddard III, W. A. *J. Phys. Chem. A* **2005**, *109*, 493.
(26) Cheung, S.; Deng, W.; van Duin, A. C. T.; Goddard III, W. A. *J. Phys. Chem. A* **2005**, *109*, 851.
(27) van Duin, A. C. T.; Zeiri, Y.; Dubnikova, F.; Kosloff, R.; Goddard III, W. A. *J. Am. Chem. Soc.* **2005**, *127*, 11053.
(28) Kerr, J. A.; Sekhar, R. C.; Tromtman-Dickenson, A. F. *J. Chem. Soc.* **1963**, 3217.

JP900194D